**Proceedings of ICONE14**
**International Conference on Nuclear Engineering**
**July 17-20, Miami, Florida, USA**

# ICONE14-89044

# APERIODIC INSTABILITY OF A ONCE-THROUGH STEAM GENERATOR WITH A FEEDWATER LINE

**Jae-Kwang Seo, Han-Ok Kang, Juhyeon Yoon, Keung-Koo Kim**

Fluid Engineering Division
Korea Atomic Energy Research Institute
150, Dukjin-dong, Yuseong-gu, Daejeon, Korea

## ABSTRACT

Aperiodic (static) flow instability is an instability related to the change of a flow direction in individual steam generating U-shaped channels operating at given pressure difference. The nature of an aperiodic instability is close to a Ledinegg instability [1] related to the presence of multiple flows at the full hydraulic curve of a U-shaped channel. In this paper, the conditions for a reverse flow for a once-through steam generator (OTSG) with U-shaped modular feedwater line (MFL) are studied. From the results of the studies, it is revealed that the change of a flow direction in the MFL is due to the boiling of the feedwater in the downcomer branch of the U-shaped MFL and that multiple flows start in an area of the extremes corresponding to the minimum pressure difference of the hydraulic curves. Calculation models for predicting a threshold of an aperiodic instability for the OTSG of interest is proposed and the analysis results are compared with the experimental data.

## INTRODUCTION

The hydrodynamic stability of OTSG, in particular OTSG in nuclear power plant, is one of the most important conditions ensuring their reliable operation. The operation of a OTSG under unstable conditions can damage the heating surface as a result of overheating or temperature fluctuations, and lead to a decrease of the heat reception [2].

It is known that two types of instability are possible for the OTSG [3]: a parallel-channel instability in the system of the channels connected in parallel and an aperiodic instability in the system of the U-shaped channels:

Hydrodynamic instability of the OTSGs in terms of steam-water flow fluctuations occurs in the system of parallel channels and operating at a permanent pressure difference. It should be noted that it is typical for the OTSG to operate in low flow and low pressure conditions. The main disturbance source in a steam-water channel, finally leading to flowrate fluctuations, is the steam generation area at the beginning of the evaporating section. One of the most evident ways to ensure a stable operation of the parallel steam generating channels is the installation of orifices at the channel inlet. It is evident that due to an increase of the inlet orifice, i.e. hydraulic resistance of the section with a single-phase fluid, the relative disturbance of the pressure difference at the beginning of the steam generation section decreases and thus it represents a stabilizing effect. It is also well known that the factor influencing the occurrence and progress of parallel-channel flowrate fluctuations include: a decrease of the fluid mass velocity, increase of the heat flux, and a pressure decrease [4]. Recommendations on an assurance of a stable curve of the steam generating channel were developed on the basis of theoretical study results, performed by such known authors as P. A. Petrov [5]. So, for example, Petrov's criterion is a widely used criterion to determine the operation stability of the OTSG:

$$K_{orifice} = \frac{\Delta P_{orifice} + \Delta P_{economizer}}{\Delta P_{evapor} + \Delta P_{steam}} \geq 1$$

where $K_{orifice}$ is called an orifice coefficient and $\Delta P_i$ is hydraulic resistance of i section. Application of Petrov's criterion as one of the factors for the evaluation of the flow stability boundaries for facilities similar to the studied ones is quite justified and it seems highly convenient. However reference 3 states that further studies have shown that the value of an orifice coefficient, where a stable operation of the steam generating channels is assured, could vary within a wide range for various facilities and that the results of the experimental studies performed by different authors demonstrated that the application of an orifice coefficient for the analysis of a channel hydrodynamic stability is possible for heated surfaces similar to those studied for the layout and operation conditions.

Aperiodic instability is an instability with the flow oscillations in a phase shift of $180^\circ$ at some individual channels. Depending on the channel design, parameters of the primary and secondary circuits and the plant operation mode,

an aperiodic instability can be characterized by the following phenomena:

- reversed circulation (change of flow direction to opposite direction) or a circulation stagnation in individual steam generating channels;
- aperiodic changes of the flowrate in the steam generating channels (process of a reversed circulation with a subsequent recovery progress without a certain period);
- fluctuations of the secondary fluid flowrate in the channels with the amplitude of 100% and a rather stable period.

For the OTSGs the danger of an aperiodic instability is mainly related to a thermal cycling of the feedwater pipes, headers, pipe sheets and other structural components of the pipe system such as the welds and complicated profiles. The study of a flow stability in parallel channels with a riser-downcomer fluid movement was first carried out for the models of once-through fossil fuel boilers. The most important work direction was to study the conditions for a flow reversed circulation. By neglecting an external driving force, multiple flows start in an area of the extremes corresponding to the minimum pressure difference of the hydraulic curves. Equation of a full hydraulic curve is as follows:

$$\Delta P_{\Sigma} = P_{water} - P_{steam} = \Delta P_h - H$$

where $\Delta P_h$ is the total hydraulic resistance of the system of the SGC. H is the full hydrostatic head between the headers, which equals the difference of the hydrostatic heads of the downcomer and riser sections. If a full hydraulic curve is located in quadrants I, III and IV, it has two characteristic points (Fig. 1) :

$Ffw_{boundary}$ = boundary flowrate where an equality between the hydraulic resistance and the leveling pressure head of the module is achieved;

$Ffw_{boiling}$ = flowrate where a feedwater boiling starts at the upstream of the orifice or the orifice itself.

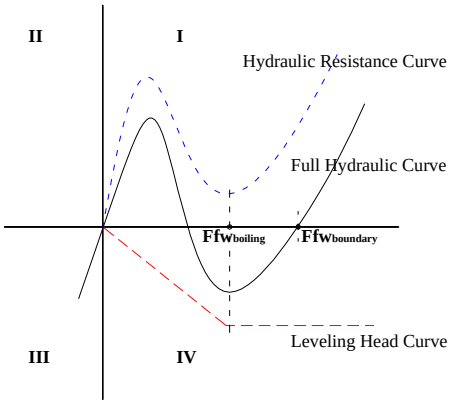


Fig. 1. Hydraulic Curve of U-Shaped Steam Generating Channel of the OTSG

In quadrant I the full hydraulic curve is a single-valued and it ensures an absence of an aperiodic instability. The curve with such a shape is possible in emergency cooldown modes at a low steam pressure. It may also be observed for a short period of time in heatup conditions. At the flowrate $Ffw < Ffw_{boundary}$ the curve transfers to quadrant IV in the range of multiple flowrates. A stable steam generator operation can be ensured in the range of flowrates $Ffw_{boiling} < Ffw < Ffw_{boundary}$, especially if the working point is at a far distance from point $Ffw_{boiling}$, i.e. there is a sufficient enough margin till the feedwater boiling upstream of the orifice or in the orifice itself. In quadrant III the curve describes the reverse steam movement from the steam header to the water one. Transfer from quadrant III to IV of the hydraulic curve and vice versa means the start of a steam generator aperiodic instability. In this study mathematical models for predicting the temperature distribution and the pressure distribution along a secondary fluid flow path are proposed and by using the models we will establish the conditions for a flow reversed circulation for the OTSG with the MFLs enclosed by an enclosure assembly. Finally the experimental results will be explained with the analysis results.

## NOMENCLATURE

$A$: heat transfer area, $m^2$
BBM: bottom bared MFL
$d$: diameter of the tube, m
$\bar{d}_z$: average diameter of coiling, m
$dP$ (DP): differential pressure, kPa
DT: subcooled margin at orifice, ℃
F: (normalized) flowrate, (%) kg/s
fw: feedwater
$h$: heat transfer coefficient, $W/m^2K$
$H$: enthalpy, J/kg
HA: horizontal assembly
HTC: heat transfer coefficient
$k$: thermal conductivity, W/mK
$K_{orifice}$ (Korifice): orifice coefficient
$\dot{m}$ : mass flowrate, kg/s
MFL: modular feedwater line
MSL: modular steam line
NA: nozzle assembly
$T$: coolant temperature, ℃
$N$: number of modular feedwater (steam) lines
$N_t$: number of the SGC tubes
OTSG: once-through steam generator
$P$: pressure, MPa
$U$: overall heat transfer coefficient, $W/m^2K$
$U_L$: linear heat transfer coefficient, W/mK
$\dot{Q}$: thermal power, W
RC: reactor (primary) coolant
SG: steam generator
SGC: steam generator cassette
TBM: top bared MFL
VA: vertical assembly
$\eta$ : (heat transfer) area safety factor

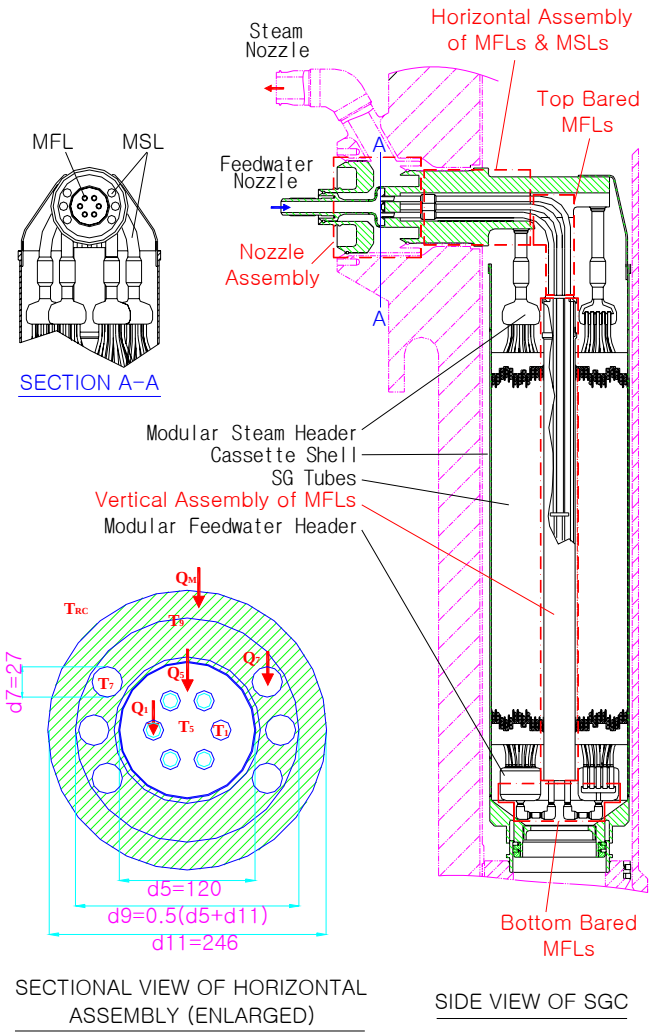


Fig. 2. The SGC with a Sectional View of the Horizontal Assembly of the MFLs and MSLs

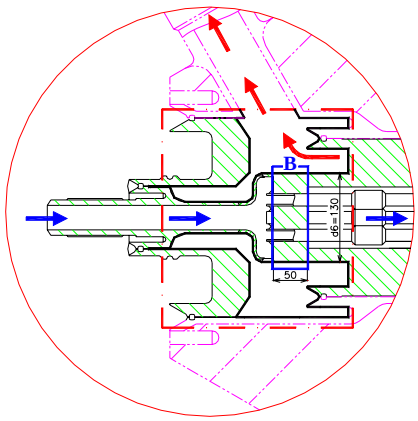


Fig. 3. Detail of the Nozzle Assembly

## MATHEMATICAL MODELS

In order to predict a threshold of an aperiodic instability for the SGC of interest, it is necessary to develop a model of the thermal hydraulic analysis for various types of enclosure assemblies which are enclosing the MFLs. The enclosure assembly of the MFLs is designed to aim at the purpose of a stabilizing effect of the secondary system by a reduction of the heat transfer from the hot primary side to the cold feedwater side.

### General Description for Various Types of Enclosure Assemblies of the MFLs along a Flow Path

Steam generator cassette (SGC) of interest in this study is a once-through modular type and it is installed inside the reactor vessel of an integral type reactor. Modular feedwater line (MFL) penetrates the upper part of the reactor vessel side wall and is connected to the bottom head of the SGC. Modular steam line (MSL) also penetrates the upper part of the reactor vessel side wall and it is connected to the top head of the SGC (Fig. 2). One SGC consists of six MFLs and six MSLs. Schematically, as seen from the SGC sectional view, the secondary circuit of each module represents a U-shaped channel formed by the MFL located at the downcomer section and the active part of the SGC located at the riser section. With such a geometrical configuration of a long U-shaped channel of the MFL, a sufficient heating of the feedwater in the MFL may cause an aperiodic flow instability especially at low flow and low pressure conditions. Due to the design characteristics of the MFL and MSL layout, the MFLs are enclosed by various types of cylindrical heat structures (called an enclosure assembly or shortly an assembly) along a flow path.

The geometrical flow structure of the Nozzle Assembly (NA) is quite complex. The MFLs are enclosed by a thick cylindrical metal enclosure over which a bulk steam flows. With such a geometrical configuration, there can be a huge amount of the heat loss from the steam to the feedwater in the MFLs at the NA, resulting in a degradation of the steam quality (or superheat) from the SGC tube exit and in an increase of the feedwater temperature.

At downstream of the NA before a turning of the feedwater flow to downward direction, the MFLs are enclosed by the Horizontal Assembly (HA) of hollow cylinder, inside which a nearly stagnant water exists and in which six holes of the MSLs penetrate. The stagnant water inside the HA functions as a thermal barrier against a heat transfer from a hot side of the primary coolant to a cold side of the feedwater. A sectional view of the HA is shown in the bottom-left area of Fig. 2.

The Vertical Assembly (VA) consists of the MFLs, a nearly stagnant water, and a thin hollow metal cylinder.

Due to difficulty of manufacturing problem, there are two regions of the MFLs which are not enclosed by an enclosure assembly: Top Bared MFLs (TBM) and Bottom Bared MFLs (BBM). Huge amount of a heat is transferred to the feedwater through these bared MFLs.

**Heat Balance Equations for the NA**

At the region of the NA, a steam from the MSLs directly contacts the wall surface of the NA. In order to predict an accurate heat transfer quantity through the heat transfer surface of the NA, rigorous 3-dimensional thermal hydraulic analysis may be needed. Total heat transfer area of the NA may be divided into several sub domains depending on the local shape of the heat transfer structure. In this study, heat transfer characteristics of the NA are assumed to be represented by region B, as shown in Fig. 3., with a proper extension of the heat transfer area for a calculation simplicity. Then, a heat balance equation can be setup as follows by using the concept of a total resistance between the steam and the feedwater:

$$R_6 = \frac{1}{h_1 A_1} + \frac{1}{kS} + \frac{1}{h_6 A_6}$$

$$\dot{Q}_1 = \dot{m}_1 dH_{\ 1}$$

$$\dot{Q}_6 = \dot{m}_1 dH_{\ 6}$$

$$S = \frac{N\, 2\pi L}{\ln(\frac{d_6}{d_c}) - \frac{1}{N}\ln(\frac{N d_1}{d_c})}$$

Shape factor S is based on reference 6. L is the axial length of the heat transfer region B, $d_1$ is the inner diameter of one MFL, $d_c$ and $d_6$ are respectively the concentric and the outer diameter of the enclosure of interest.

**Heat Balance Equations for the HA**

A heat balance equation for N tubes in the HA can be written as follows:

$$\dot{Q}_1 = \dot{m}_1 dH_{\ 1}$$

$$d\dot{Q} = \dot{Q}_5 - N\dot{Q}_1 = \dot{m}_5 dH_{\ 5}$$

$$\dot{Q}_9 - \dot{Q}_5 = N\dot{m}_7 dH_{\ 7}$$

$$\dot{Q}_1 = U_{14} A_1 \Delta T_{15}$$

$$\dot{Q}_5 = U_{59} A_5 \Delta T_{59}$$

$$\dot{Q}_7 = U_{78} A_7 \Delta T_{78}$$

$$\dot{Q}_9 = U_{911} A_9 \Delta T_{911}$$

where the subscripts 4 and 9 mean the outer surface $d_4$ of the one MFL and the average diameter $d_9$ of the enclosure assembly respectively. It is assumed that $T_9$ represent the average temperature of a hatched area of the metal structure of the HA. The meaning of the number in the subscript is shown in Fig. 2. $d_8$ is the equivalent concentric diameter of the enclosure assembly and defined as follows:

$$d_8 = F \cdot \sqrt{\frac{4}{N\pi} A_{hatched} + d_7^2}$$

$$A_{hatched} = \frac{\pi}{4}(d_{11}^2 - d_5^2)$$

where F is the geometrical shape adjustment factor. Since $d_8$ is located inside the hatched area, $T_8$ can be set equal to the representative metal temperature of $T_9$.

**Heat Balance Equations for the VA**

A heat balance equation for N tubes in the VA can be written as follows:

$$\dot{Q}_1 = \dot{m}_1 dH_{\ 1}$$

$$d\dot{Q} = \dot{Q}_5 - N\dot{Q}_1 = \dot{m}_5 dH_{\ 5}$$

$$\dot{Q}_1 = U_{14} A_1 \Delta T_{15}$$

$$\dot{Q}_5 = U_{56} A_5 \Delta T_{56}$$

where the subscript 6 means the outer diameter $d_6$ of the thin hollow cylindrical enclosure assembly.

**Heat Balance Equations for the TBMs and the BBMs**

A heat balance equation for a single pipe can be applied as follows:

$$\dot{Q}_1 = \dot{m}_1 dH_{\ 1}$$

$$\dot{Q}_1 = U_{14} A_1 \Delta T_{14}$$

where the subscript 4 means the hot reactor coolant region outside the pipe.

**Heat Balance Equations for the SG tube**

A modular OTSG with a helical heat transfer surface consists of several modules connected in parallel. In this analysis it was assumed that the primary and secondary water are distributed uniformly in the modules. The analysis involves an integration of the following parameters along the length of the SG tube:

- tube side (secondary coolant) enthalpy $H_S$
- shell side (primary coolant) enthalpy $H_P$
- thermal power of one cassette $\dot{Q}$

$$\frac{dH_S}{dz} = \frac{U_{PS} \cdot \pi \cdot d_S (T_P - T_S)}{\dot{m}_S} N_t \eta$$

$$\frac{dH_P}{dz} = \frac{U_{PS} \cdot \pi \cdot d_S (T_P - T_S)}{\dot{m}_P} N_t \eta$$

$$\frac{d\dot{Q}}{dz} = U_{PS} \cdot \pi \cdot d_S (T_P - T_S) N_t \eta$$

where the subscript S, P, and z mean secondary side, primary side, and flow direction, respectively.

Depending on the secondary water enthalpy, the SG tube can be divided axially into the following parts: economizer part; evaporation part; steam superheating part. At each part, the heat transfer is calculated by its own correlations recommended by the SG designer [7]. Heat equations are solved together with a hydraulic path equation for the secondary water.

It is also necessary to take into account the heat transfer intensity coefficient due to the helical coiling effect, which is multiplied by the secondary side heat transfer coefficient:

$$\varepsilon = 1 + 3.54 \frac{d_S}{\bar{d}_Z}$$

where $\bar{d}_Z$ is average diameter of coiling of the SG tube.

**Overall Heat Transfer Coefficient**

Overall heat transfer coefficient for various hollow cylindrical structures is defined as follows:

$$U_{ij} = \frac{1}{\frac{1}{h_i} + \frac{0.5 d_i}{k} \ln \frac{d_j}{d_i} + \frac{0.5 d_i}{k_{eff}} \ln \frac{d_j + d_{gap}}{d_j} + \frac{d_i}{d_j h_j}}$$

where $d_{gap}$ is a stagnant water thickness between $d_j$ and the nearby metal structure of the reactor vessel. where i and j means normally the inside region and the outside region of the structure, respectively. If i (or j) indicates a metal itself, then $h_i$ (or $h_j$) get infinite. If there is no stagnant water gap, then $k_{eff}$ get infinite.

**Flow-Pressure Drop Equation**

$$-\frac{dP}{dz} = \left(\frac{dP}{dz}\right)_{acc} + \left(\frac{dP}{dz}\right)_{fric} + \left(\frac{dP}{dz}\right)_{form} + \left(\frac{dP}{dz}\right)_{gravity}$$

The homogeneous equilibrium model is used for the calculation of the pressure drop.

**Heat Transfer Coefficient Correlations**

Empirical correlations used in this study for the heat transfer coefficients (HTCs) for various regions are summarized in Table 1. Subcooled nucleate boiling on the inner wall surface of the MFL and a steam condensation on the outer wall surface of region B should be considered. Heat transfer mechanism at the very thin gap between the enclosure and the reactor vessel wall is essentially a natural convection and therefore it is modeled as an effective conduction. There may be a bypass flow inside the enclosure and therefore it may be modeled as a forced, mixed, or natural convection, depending on the flow conditions.

Table 1. Empirical Correlations for the HTCs

| Location | HT regime | Correlations |
|---|---|---|
| Single pipe inside or outside, $d_1$ | Forced convection | Dittus [6] |
| SG tube inside (single phase flow region), $d_S$ | Forced convection | Dittus [6] |
| SG tube inside (two phase flow region), $d_S$ | Bulk boiling | SKBK [7] |
| SG tube shellside, $d_P$ | Forced convection | SKBK [7] |
| VA outside, $d_6$ | Forced convection | Dittus [6] |
| HA/VA inside, $d_4$ | Mixed or NC | Kutateladze [8] |
| HA (I) outside, $d_{11}$ | Effective | Mikheev [9] |
| HA (II) outside, $d_{11}$ | Forced convection | Dittus [6] |
| MFL/TBM/BBM, $d_1$ | Partial SNB | Rohsenow [10] |
| MFL/TBM/BBM, $d_1$ | Onset of SNB | Bergles [11] |
| MFL/TBM/BBM, $d_1$ | Fully developed | Bergles [11] |
| Region B outside, $d_6$ | Single phase/ condensation | Dittus [6]/ Shah [12] |

Note) HT = heat transfer, NC = natural convection, SNB = subcooled nucleate boiling.

**Numerical Solution Procedures and Boundary Conditions**

All those equations proposed in this study are solved by the procedure as shown in a simplified algorithm (Fig. 4). It is worth noting that numerical advancing directions of the thermal loop and the pressure loop are different due to a discrepancy of the location of available boundary conditions. Boundary conditions used in the analysis are summarized in Table 2. The HA is divided into two regions depending on boundary conditions. The HA (I) is buried in the RV and there is a very thin gap between them. HA (II) is exposed directly to the reactor coolant. Bypass flow through the enclosure is assumed to be 0.1% of the nominal flow of a primary coolant.

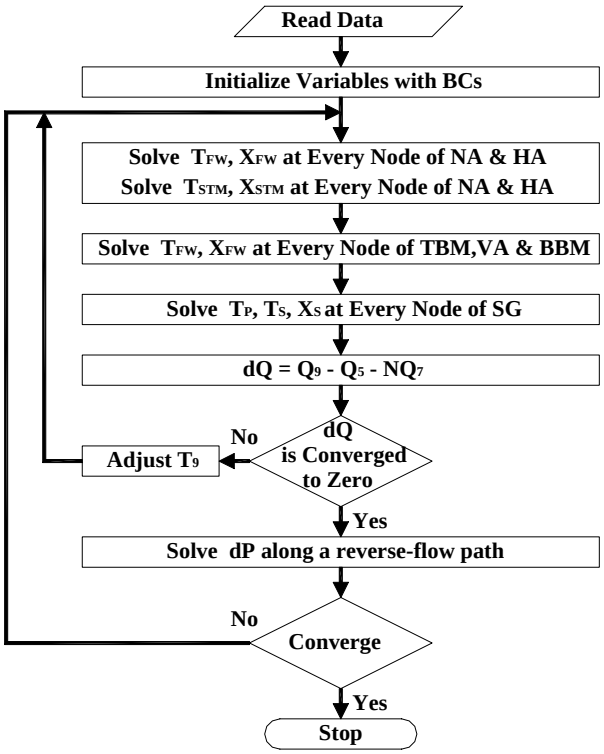


Fig. 4. Simplified Numerical Solution Algorithm

Table 2. Boundary Conditions Used in the Analysis

| Location | Boundary conditions |
|---|---|
| Feedwater nozzle | Feedwater temperature at nozzle inlet |
| HA(I) | RC temperature near wall |
| HA(II) | RC temperature near wall |
| TBM | RC temperature near wall |
| VA | Average RC temperature near wall |
| BBM | RC temperature near wall at SG outlet |
| SG | RC temperature at SG inlet |
| Steam nozzle | Steam pressure at nozzle outlet |

Table 3. Dimensional Data of the SGC

| MFL, MSL, ENC, orifice, | | SG tube | |
|---|---|---|---|
| $d_1$, MFL inner dia, m | 0.013 | No of MFLs/SGC | 6 |
| $d_4$, MFL outer dia, m | 0.018 | No of tube/MFL | 16 |
| F, HA shape factor | 0.7 | $d_S$, inner dia, m | 0.007 |
| NA effective length, m | 0.36 | $d_P$, outer dia, m | 0.01 |
| ENC metal k, W/mK | 16.3 | Lateral pitch, m | 0.014 |
| HA(I) length, m | 0.2 | Vertical pitch, m | 0.0115 |
| HA(II) length, m | 0.2 | Active height, m | 1.117 |
| TBM length, m | 0.3 | Tube material | Ti |
| VA length, m | 1.6 | Roughness, m | 3E-5 |
| BBM length, m | 0.25 | Helical dia, m | 0.268 |
| $dP_{MSL}$ at NDP, MPa | 0.05 | Tube length, m | 10.23 |
| $dP_{MFL\ Fitting}$ at NDP, MPa | 0.017 | Area safety factor | 0.95 |
| $dP_{orifice}$ at NDP, MPa | 0.913 | | |

Note) ENC = enclosure, NDP = nominal design point.

Table 4. Analysis Cases for an Aperiodic Flow Instability

| Cases | F1, % | Ffw, % | T1, ℃ | Tfw, ℃ | Pstm, MPa | Results | |
|---|---|---|---|---|---|---|---|
| | | | | | | Analysis | Experiment |
| I | 100 | 1~20 | 310 | 50 | 3.45 | Fig. 5 | None |
| II | 100 | 1~20 | 310 | 140 | 3.40 | Fig. 6 | Fig. 12 |
| III | 50 | 1~20 | 310 | 50 | 1.6 | Fig. 7 | Fig. 13 |
| IV | 15 | 1~20 | 310 | 140 | 3.45 | Fig. 8 | Fig. 14 |
| V | 100 | 1~20 | 240 | 140 | 2.0 | Fig. 9 | Fig. 15 |
| VI | 15 | 1~20 | 240 | 140 | 2.0 | Fig. 10 | Fig. 16 |

Note) the meaning of parameters is shown in Fig. 11.

## RESULTS AND DISCUSSIONS

Based on the heat transfer and pressure drop models developed in this study, calculations have been conducted to predict the $Ffw_{boiling}$ and $Ffw_{boundary}$ and subcooled margin at the MFL header of the SGC for a given orifice coefficient $K_{orifice}$. Dimensional data except for those shown in Fig. 2 is summarized in Table 3. We selected 6 cases for the aperiodic instability analysis by considering actual operational conditions. These cases are given in Table 4.

The $K_{orifice}$ is varied with the feedwater flowrate due to a change of the boiling height in the OTSG. Sufficient water level in the economizer region of the OTSG increases the single-phase friction, which provides a damping effect on the flow disturbance and thereby increases the parallel-channel stability. Limiting amplitude of the flow oscillation for the OTSG during a normal operation is known to be about 15 ~ 20% [3]. At low flow conditions a parallel-channel oscillation can be intensified over the allowable limit. The allowable $K_{orifice}$ should be sufficient enough for the case of the geometric and thermal-hydraulic complexity involved in the system.

Fig. 5 shows the full hydraulic curve, subcooled margin at the orifice, and the $K_{orifice}$ for Case I. From Fig. 5, $Ffw_{boiling}$ and $Ffw_{boundary}$ are around 4.2% and 9%, respectively. Therefore in order to prevent an aperiodic instability, the minimum load should be greater than 4.2%. It may be recommended to operate it at 10% for an assurance. At $Ffw_{boiling}$, the subcooled margin of DT at the orifice becomes zero and the full hydraulic curve and the $K_{orifice}$ vary rapidly due to a boiling in the MFL.

The results of Case II (Fig. 6), which is the same condition as Case I except mainly for the feedwater temperature change and slightly for the steam pressure change, show the feedwater temperature effect on the system instability. It increases the $K_{orifice}$ by about 2% ~ 4% depending on loads and therefore it makes slight changes on a dynamic stability of the system. $Ffw_{boiling}$ and $Ffw_{boundary}$ are around 7.4% and 8.5%, respectively. From the point of view of an aperiodic instability, an increase of the feedwater temperature restricts the allowable range of the operations.

Peak dP after a boiling in the NFL occurs during two-phase conditions due to the combination effect of a two-phase frictional pressure drop and the hydrostatic head of a two-phase fluid column of the U-shaped MFL. Peak pressures tend to occur near high quality zone as shown in subsequent figures of results.

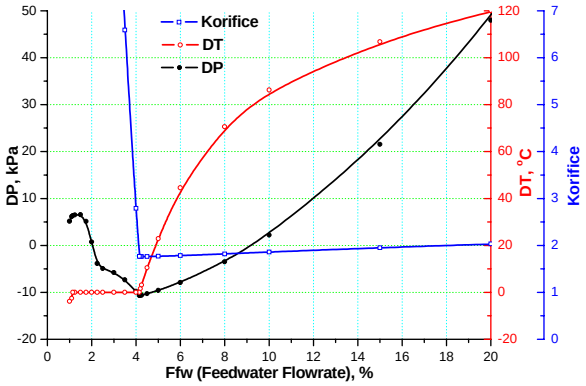


Fig. 5. DP (Full Hydraulic Curve), DT (Subcooled Margin), and $K_{orifice}$ (Orifice Coefficient) for Case I Given in Table 4

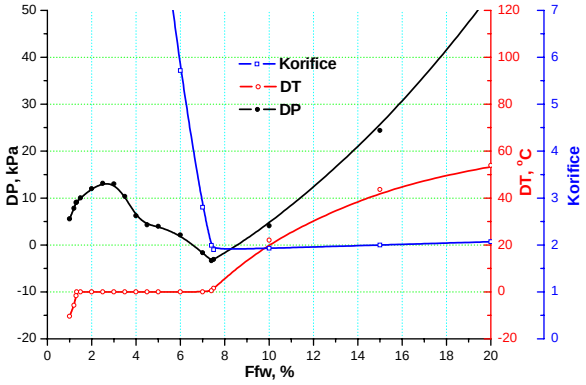


Fig. 6. DP, dT, and $K_{orifice}$ for Case II Given in Table 4

The results of Case III (Fig. 7) show a combined effect of the steam pressure reduction and the primary coolant flow reduction on the system instability. Compared to Case I, both aperiodic and dynamic instabilities get worse even though the heat addition from the primary coolant to the feedwater decreases due to the reduction of the primary coolant flowrate. This is due to the fact that a decrease of the system pressure at a given power input enhances the void fraction and thus the two-phase flow and the momentum pressure drop. These effects are similar to that of an increase of the power input or a decrease of the flowrate, and thus they destabilize the system. Petrov's criterion is not satisfied with Case III, which means that the parallel channel instability is expected to be intensified at the conditions of a low steam pressure and a high primary coolant temperature. At low steam pressure conditions, the full hydraulic curve is positive for the whole range of the load and the $K_{orifice}$ for Case III is less than unit even at 20% load. These result from an increased frictional pressure drop in the SGC tube and the MSL due to a reduced steam density. As a result, $Ffw_{boiling}$ rises to 7.3%.

A reduction of the primary coolant flow will stabilize the system because it reduces the heat addition to the system. Case IV is the same as Case II with the exception of the primary coolant flowrate, which is reduced to 15% of the nominal value. From Fig. 8, $Ffw_{boiling}$ and $Ffw_{boundary}$ are around 4.6% and 8.5%, respectively. Close comparison of Case II with Case IV reveals that at a low primary flow, the system is stabilized in both aperiodic and parallel-channel instability. The reduction of the primary flow tends to decrease the void fraction in the system and thus to retard the onset of a boiling in the MFL.

Fig. 9 shows the analysis results of Case V in the situation of a reduction of both the primary coolant temperature and the steam pressure. The former is a stabilizing contributor but the latter is a destabilizing one. Due to the reduction of the primary coolant temperature, the heat flux to the system is reduced and thus the boiling point tends to shift to left.

The results of Case VI (Fig. 10) are similar to those of Case V. Once again, the reduction of the primary coolant mass flux and heat flux stabilizes the system.

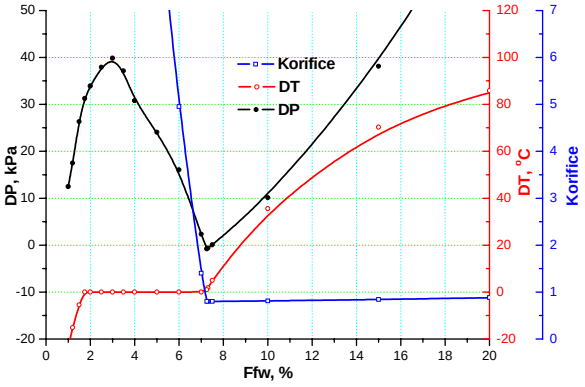


Fig. 7. DP, DT, and $K_{orifice}$ for Case III given in Table 4

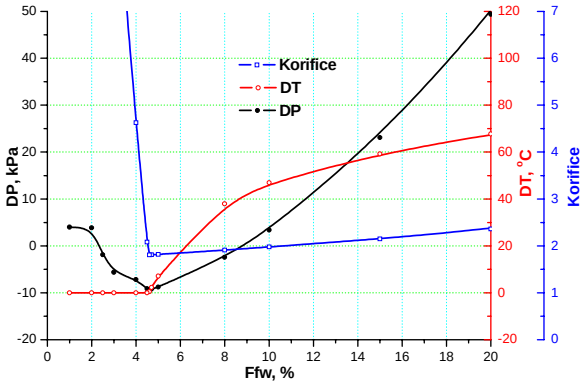


Fig. 8. DP, dT, and $K_{orifice}$ for Case IV given in Table 4

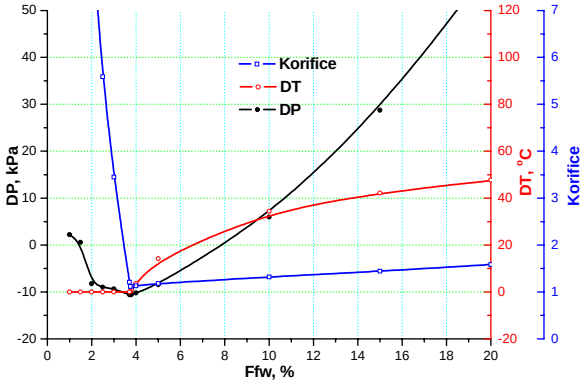


Fig. 9. DP, DT, and $K_{orifice}$ for Case V given in Table 4

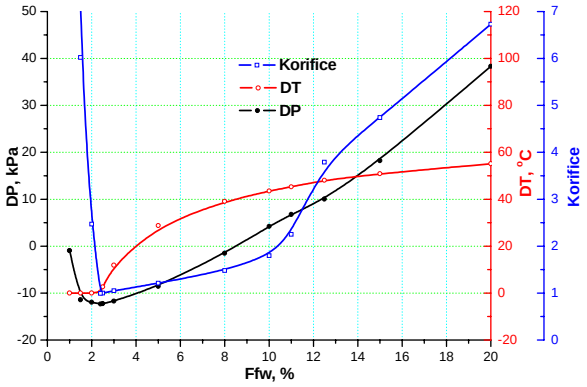


Fig. 10. DP, DT, and $K_{orifice}$ for Case VI given in Table 4

## Experimental Study on Aperiodic Instability

Experimental investigation was conducted to find a minimum allowable feedwater flowrate at the conditions given in Table 4 using a steam generator test model. The test model was developed to carry out thermal-hydraulic performance tests for the purpose of a design confirmation and an acquisition of information on limiting conditions for a safe operation of the prototype SGC. The dimensional data of the test model, which is shown in Table 3, is the same as those used in the analysis. Major measured parameters and their locations are shown in the schematic diagram of test facility (Fig. 11).

Tests were conducted at stepwise decrease (10% → 7.5 (or around 8)% → 3% → 2% → 1%) of the feedwater flowrate for all given cases. The recording of the feedwater flowrate sensor readings did not indicate any definite conclusion on the nature of hydrodynamic processes running in the test model because it is measured outside the SGC model and therefore may not be influenced by module to module and/or tube to tube flow fluctuations. As for other parameters there is an increase of relative amplitude of pressure drop fluctuations (DPII) as well as steam temperature (Tstm) fluctuations. These features are an indirect evidence of a hydrodynamic instability of the SGC.

The calculated orifice coefficient $K_{orifice}$ at 20% load is about 2.03 for Case I. The experimental result shows that relative amplitudes of pressure drop fluctuations (DPII) are about 3% at 100% load and about 10% at 20% load for Case I.

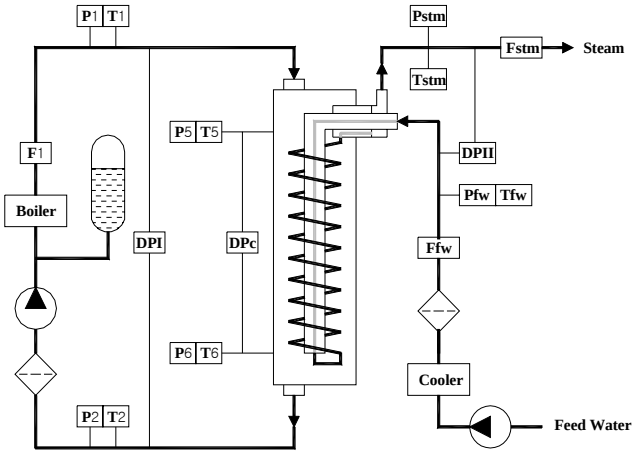


Fig. 11. Schematic Diagram of Steam Generator Test Facility

However, at flow conditions < 20% load, relative amplitudes of pressure drop fluctuations are greatly amplified as shown in Fig. 12 ~ Fig. 16.

Figures 12 a) and b) reveal that pressure drop fluctuations (DPII) for Case II are intensified but with relatively stable constant amplitude and constant period. It clearly reveals that an aperiodic instability occurs at Ffw = 3% but not at Ffw = 7.5%, which agrees well with the analytical prediction of $Ffw_{boiling}$ = 7.4%.

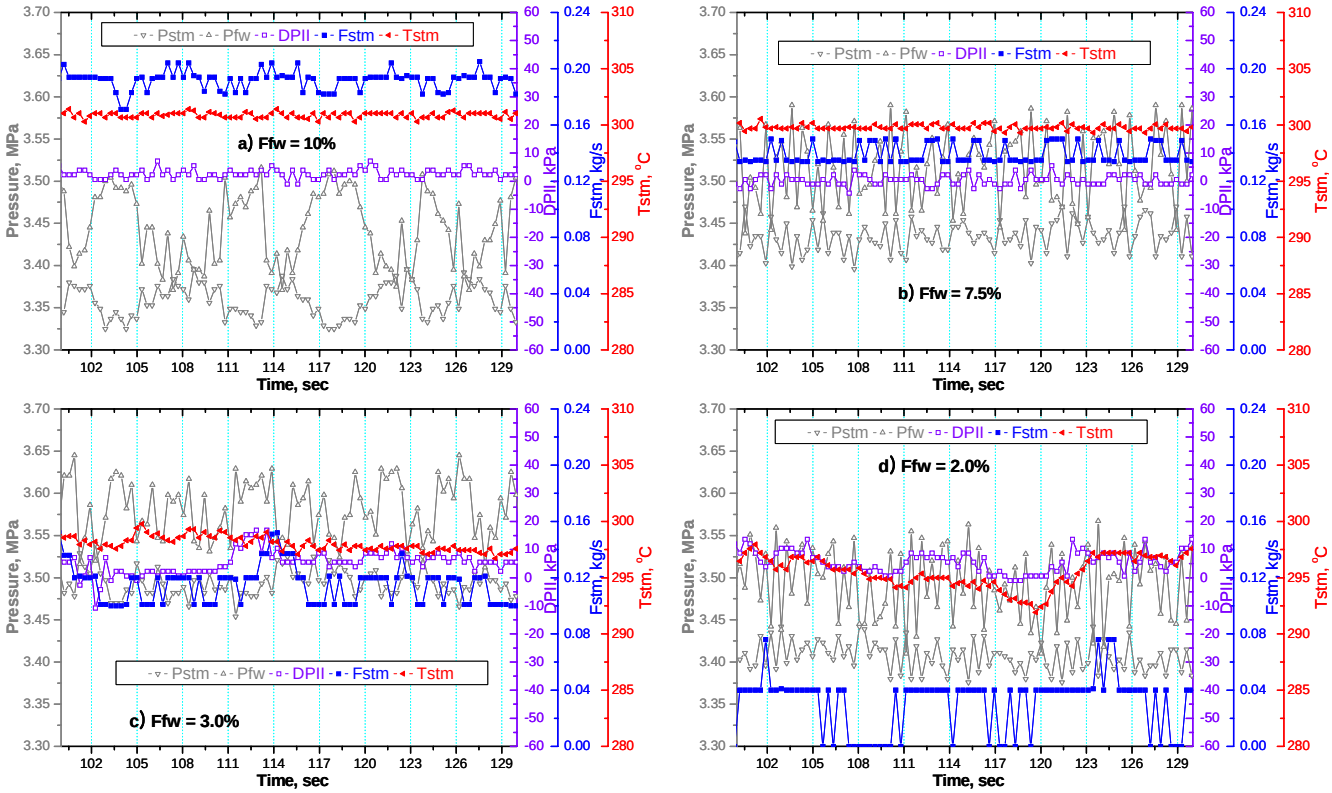


Fig. 12. Experimental Results of Case II given in Table 4

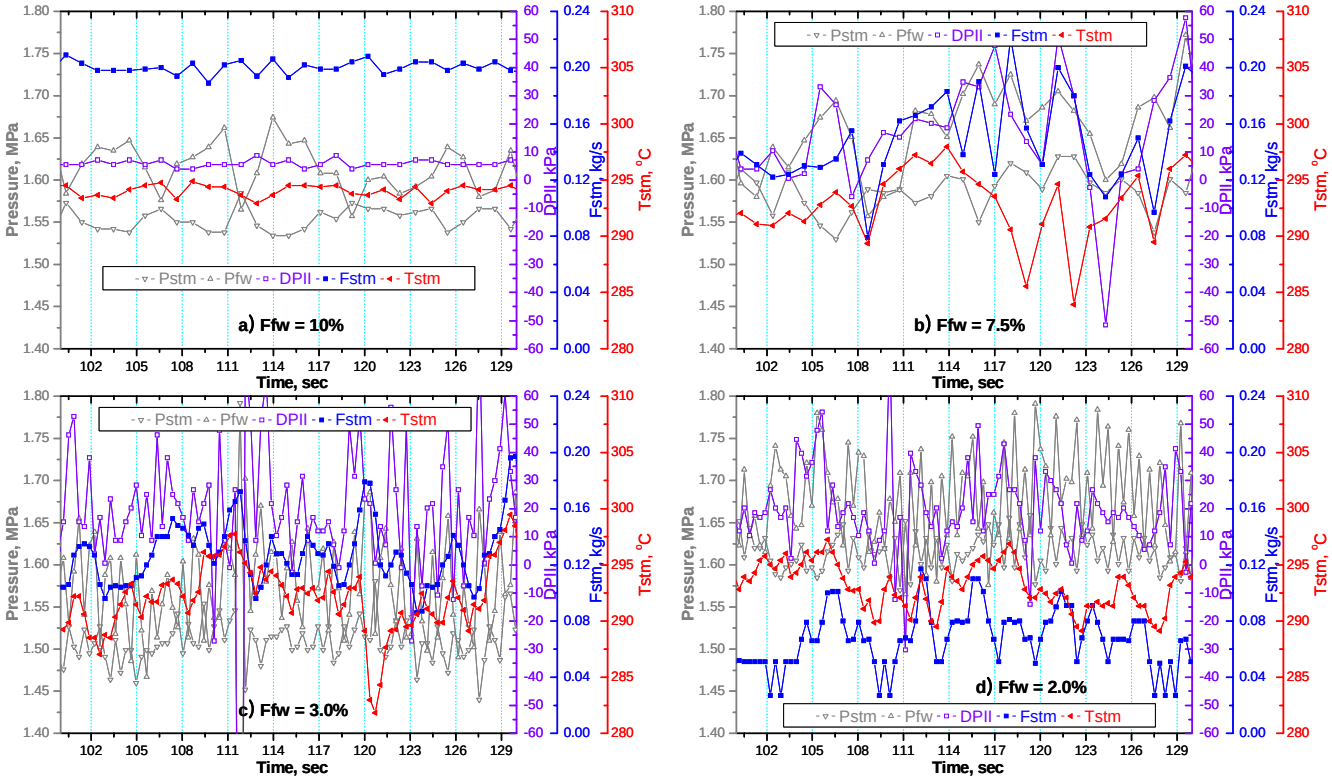


Fig. 13. Experimental Results of Case III given in Table 4

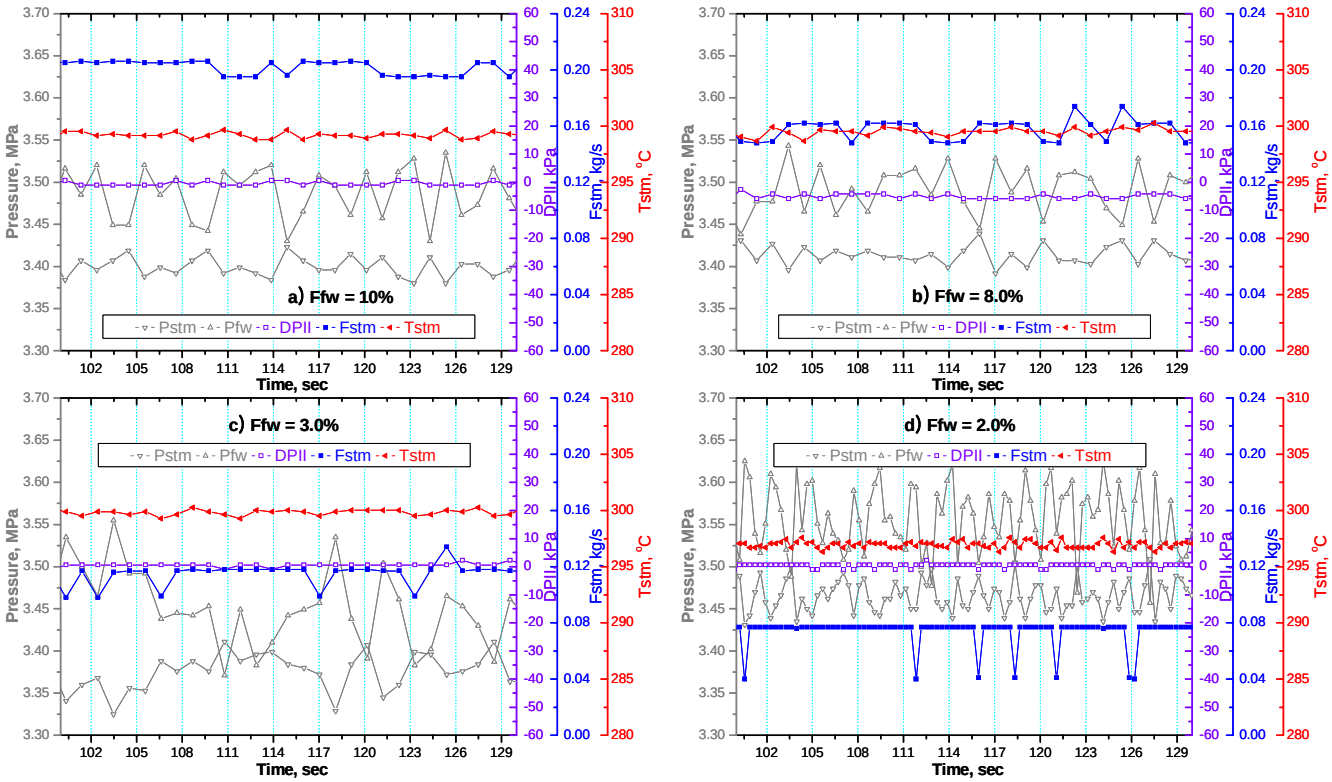


Fig. 14. Experimental Results of Case IV given in Table 4

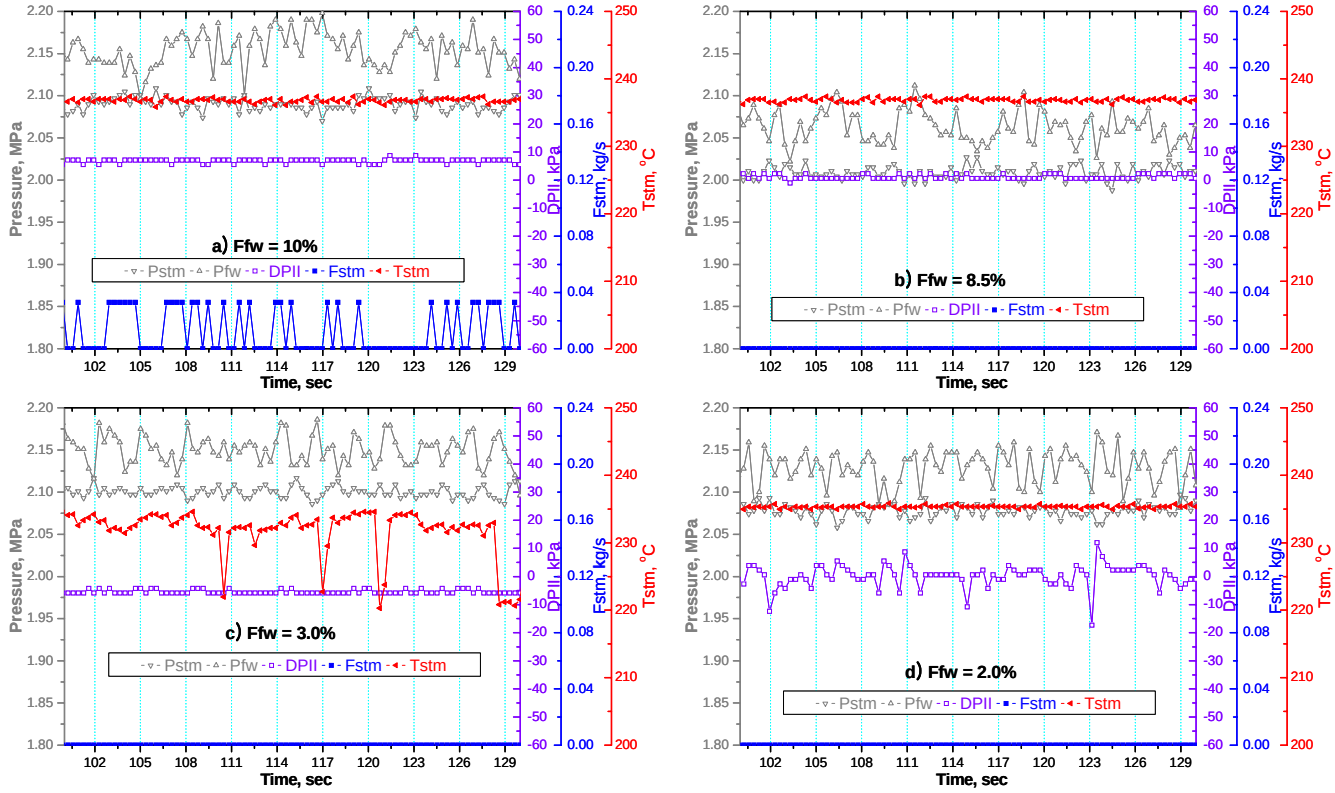


Fig. 15. Experimental Results of Case V given in Table 4

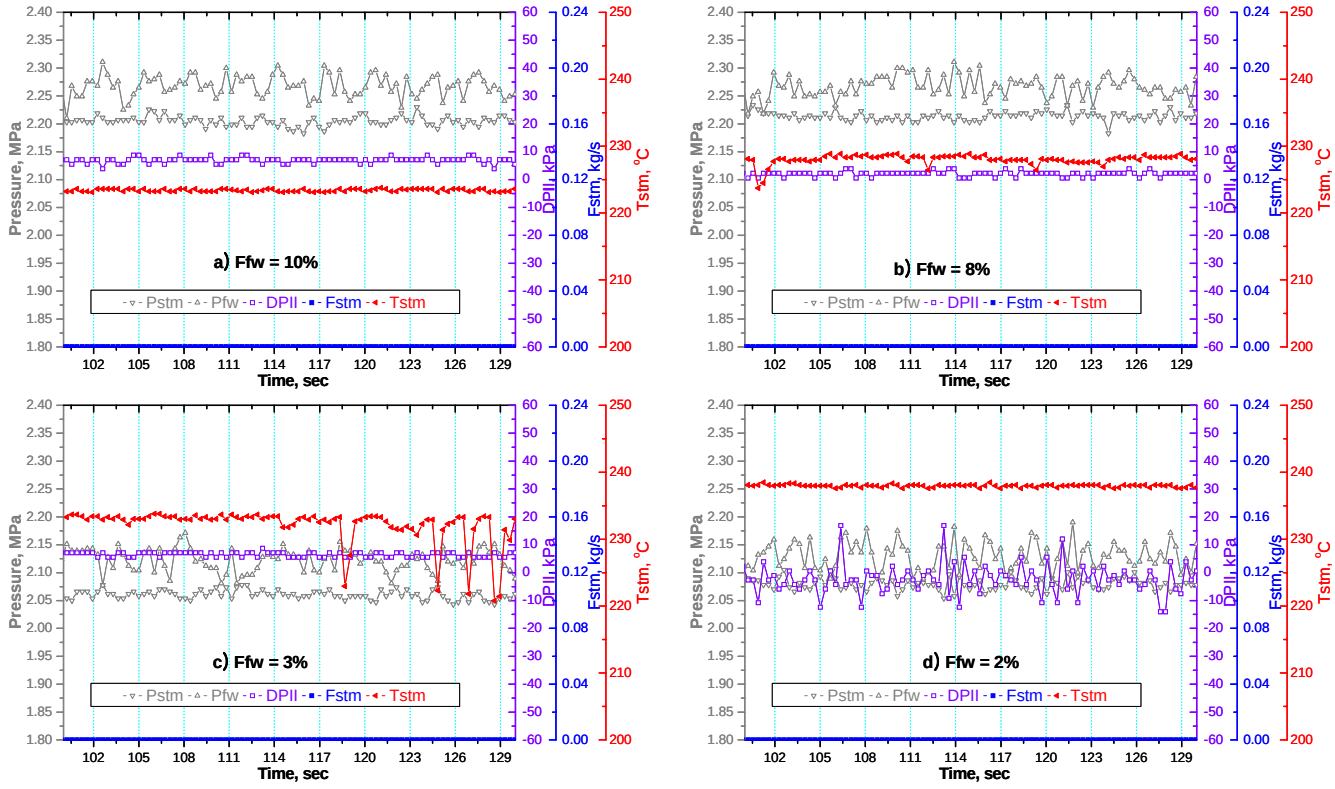


Fig. 16. Experimental Results of Case VI given in Table 4

Table 5. Summary of the Comparison of Analysis Results with Experimental Results

| Cases | Fluctuated variables | Onset of aperiodic instability | | Average of fluctuated variables | | Amplitude of fluctuated variables, % |
|---|---|---|---|---|---|---|
| | | Experiment results | Analytical prediction | Experimental results | Analytical prediction | $\left(= \frac{\text{Max} - \text{Min}}{0.5(\text{Max} + \text{Min})} \times 100\right)$ |
| II | DPII<br>Tstm<br>Fstm | **3.0%** ≤ Ffw < 7.5% | Ffw = 7.4% | DPII≈ 5 kPa<br>Tstm≈ 298 ℃<br>Fstm≈ 5.5% | DPII = 13.1 kPa<br>Tstm = 294.0 ℃ | $A_{DPII}$ ≈ 100<br>$A_{Tstm}$ ≈ 1<br>$A_{Fstm}$ ≈ 30 ~ 50 |
| III | DPII<br>Tstm<br>Fstm | **7.5%** ≤ Ffw < 10.0% | Ffw = 7.3% | DPII≈ 25 kPa<br>Tstm≈ 292 ℃<br>Fstm≈ 8.0% | DPII = 0 kPa<br>Tstm = 285.9 ℃ | $A_{DPII}$ ≈ 100<br>$A_{Tstm}$ ≈ 3<br>$A_{Fstm}$ ≈ 25 |
| IV | Tstm | **3.0%** ≤ Ffw < 8.0% | Ffw = 4.6% | Tstm≈ 300 ℃ | Tstm≈ 293.9 ℃ | $A_{Tstm}$ ≈ 3 |
| V | Tstm | **3.0%** ≤ Ffw < 8.5% | Ffw = 3.8% | Tstm≈ 227 ℃ | Tstm = 230.1 ℃ | $A_{Tstm}$ ≈ 3 |
| VI | Tstm | **3.0%** ≤ Ffw < 8.0% | Ffw = 2.4% | Tstm≈ 227 ℃ | Tstm = 230.0 ℃ | $A_{Tstm}$ ≈ 2.5 |

Fig. 13 shows that an aperiodic instability occurs at Ffw = 7.5% for Case III. This result deviated from the analytical prediction of $Ffw_{boiling}$ = 7.3% (see Fig. 7) by about 3% error.

As mentioned before the analytical prediction for the onset point of an aperiodic instability for Case IV (conditions of a reduced primary flow and an increased feedwater temperature) is about 4.6%. However there is weak indication of an aperiodic instability for Ffw=3% ~ 8%, in terms of Tstm (and maybe Fstm), from the experiment results shown in Fig. 14. However from another experimental fact that DPII at 3% is higher than that at 8%, we conclude that the onset point of an aperiodic instability may occur around the value of the analytical prediction.

Case V and VI are mild heat flux conditions in conjunction with a reduced system pressure. Experimental results (Figures 15 and 16) shows that an aperiodic instability occurs, in terms of Tstm rather than DPII, at a low flow condition of Ffw ~ 3% as predicted by the analysis result.

Table 5 shows the summary of the comparison of the analysis results with the experimental results.

## CONCLUSION

By using the thermal hydraulic models developed for understanding a flow instability known as an aperiodic instability for the system with U-shaped MFLs, full hydraulic curve with load changes is generated for various operation conditions. This curve enables us to predict the onset of an aperiodic instability for the OTSG with U-shaped MFLs.

It is revealed through a theoretical analysis that a boiling in the MFL due to an over heating of the feedwater is the main source for the occurrence of an aperiodic instability for a OTSG with U-shaped MFLs.

From the comparisons of the analysis results with the experimental results, it is concluded that a limiting load (feedwater flowrate) for a stable operation of a OTSG for a given operation conditions can be predicted by using the analysis model developed in this study.


## ACKNOWLEDGMENTS

This work was performed with financial support from the Research Fund of National Science Research Minister.


## REFERENCES


[1] Ledinegg, M., 1938, “Instability of Flow during Natural and Forced Circulation”, Die Warme 61:8, AEC-tr-1861 (1954).

[2] I. I. Belyakov, M. A. Kvetnyi, D. A. Loginov, S. I. Mochan, “Static Instability of Once-Through Steam Generators with Convective Heating”, Atomic Energy, volume 56 Issue 5, May 1984, Pages 347 – 350, DOI 10.1007/BF01124329, URL http://dx.doi.org/10.1007/BF01124329.

[3] Babin, V. A., et al., 2004, “Final Report on Problems of Ensuring the Hydraulic Stability of the OTSGs in Normal Operating Modes”, KAERI-OKBM report.

[4] Tong, L. S., and Tang, Y. S., 1997, “Boiling Heat Transfer and Two-Phase Flow”, Taylor & Francis.

[5] Petrov, P. A., 1960, “Hydrodynamics of Once-Through Boiler”, Gosenergoizat (in Russian).

[6] White, F. M., “Heat and Mass Transfer”, Addison Wesley Publishing Company, 1988.

[7] Steam Generator with Helically Coiled Heat Transfer Area, Analytical Method (IZH ER.500609.001), SKBK.

[8] Kutateladze, S. S., and Borishansky, V. M., 1959, “Handbook on Heat Transfer”, Gosenergoizdat.

[9] Mikheev, M.A., Mikheeva, I.M. “Heat Transfer Principles”, Moscow, Energia, 1973.

[10] Rohsenow, W. M., 1962, “A Method of Correlating Heat Transfer Data for Surface Boiling of Liquids”, Trans. ASME, Vol. 84, pp. 969.

[11] Bergles, A. E., and Rohsenow, W. M. “The Determination of Forced-Convection Surface Boiling Heat Transfer”, 1964, J. Heat Transfer, Vol. 86, pp. 365-372.

[12] Shah. M., “A General Correlation for Heat Transfer during Film Condensation inside Pipes”, Int. J. Heat Mass Transfer, Vol. 22, pp. 547-556, 1979.